LABORATORI NAZIONALI DI FRASCATI
SIS-Pubblicazioni

LNF-04/28 (IR)
9 December 2004

CHEMICAL AND MAGNETIC CHARACTERIZATION OF THE STEELS FOR THE OPERA SPECTROMETERS

A. Cecchetti[1], B. Dulach[1], D. Orecchini[1], G. Peiro[2], F. Terranova[1]
[1)] *INFN, Laboratori Nazionali di Frascati, Frascati, Italy*
[2)] *CERN, Geneva, Switzerland*

Abstract

A full characterization of the chemical and magnetic properties of the steels for the OPERA magnetic spectrometers has been carried out during mass production. In the following, we present the results and discuss the impact of the different steel responses on the B-field maps and on the physics performance of the detectors.

PACS:14.60Pq, 07.55Db

1 Introduction

The instrumented magnets [1,2] of OPERA act both as subdetectors and as the basic support structure of the whole experiment [3]. During the mounting of the other subdetectors (walls and target trackers) the mechanical structure of the spectrometers subdues significant stresses and, after the completion of the installation, the magnet upholds the weight of the target tracker, the magnetic forces and possible seismic stresses. As a consequence, the choice of the magnet steel is driven by severe mechanical constraints but its composition must be appropriate for magnetic applications (high magnetic permeability) in order to achieve the nominal field for deflection of charged particles. In the following we present a full characterization of the steels that have been produced for the vertical slabs and the return yokes of the magnet; we discuss the impact of steel non-uniformity on the B-field maps both in the fiducial region of the spectrometer (vertical slabs housing the active detectors) and in the area of the return paths.

2 Steel specifications and chemical analysis

In order to cope simultaneously with the magnetic and mechanical requirements, a S235 JR steel (unalloyed steel for magnetic application) in compliance with UNI EN 10025 has been chosen. In addition, upper limits on the weight fractions for C, P and S has been specified (see column 2 of Tab.1). Different producers were selected for the slabs and the return yokes (RY). The slabs were produced by DUFERCO, Clabecq, Belgium. Machining has been carried out by MELONI, Tivoli (RM), Italy. The return yokes were produced and machined by FOMAS, Osnago (LC), Italy. The chemical analysis was done by the steel producers on a heat by heat basis. For the return yokes, each heat corresponds to a different magnet block and two samples per heat (sample “A” and “B”) were made available. The location of the blocks and the heat-block correspondence table can be found in Appendix A. Similar samples have been produced for the slab heats and are listed in Appendix B. The slab and RY composition is summarized in Table 1, where the mean weight fractions and the corresponding RMS are indicated for various dopants. The distribution of the weight fraction of C, P, Mn and S for the heats of the slab and return yoke steel are shown in Fig.1 and 2, respectively.

Excellent mechanical properties have been achieved for the vertical slab steel thanks to the increased Mn and C contamination. As shown in the following section, this is done at the expense of magnetic permeability. Better magnetic properties are retained by the yoke steel; this is due especially to the much lower C content. The Boron weight fraction has been kept at the level of 1 ppm in both cases. The mechanical and geometrical prop-

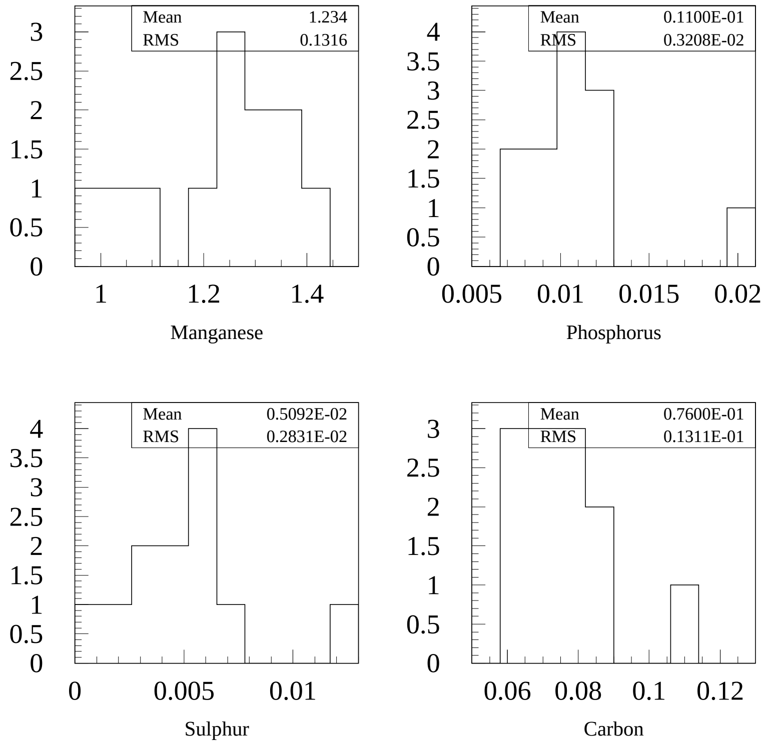

Figure 1: Distribution of the weight fraction of Mn, P, S and C for 12 different heats of the slab steel (DUFERCO). Units are in % of weight.

Element	Spec.	Slab steel	Yoke steel
C	<0.080	0.08 ± 0.01	0.005 ± 0.002
P	<0.025	0.011 ± 0.003	0.004 ± 0.002
S	<0.010	0.005 ± 0.003	0.006 ± 0.002
Mn		1.24 ± 0.13	0.24 ± 0.03
Si		0.20 ± 0.03	0.86 ± 0.05
B	<0.0005	< 0.0001	0.00011 ± 0.00004

Table 1: Average weight fraction of dopants measured after the production of the slab steel (column 3) and the return yoke steel (column 4). Column 2 shows the limits imposed to producers by tender specs. Units are in % of weight.

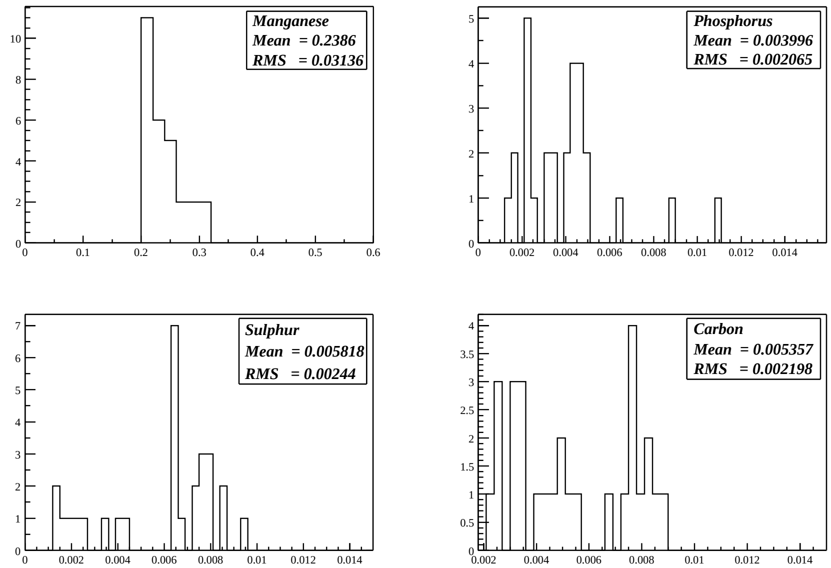

Figure 2: Distribution of the weight fraction of Mn, P, S and C for the heats of the return yokes (average over samples “A” and “B”). Units are in % of weight.

erties have been shown to be compliant with UNI EN 10025, EN 10029 and EN 10163. The main mechanical specifications requested for each heat and the corresponding post-production results are described in Ref. [3].

3 Magnetic properties

An extensive analysis of the magnetic properties of the samples has been carried out at CERN (AT-MAS). The samples have been shaped in toroids (outer diameter: 11.4 cm) so that a split-coil permeameter as developed at CERN could be used. This instrument avoids the need for a lengthy individual winding of each sample under test thus speeding up the measurements. For each sample, the first magnetization curve up to $H \simeq 24$ kA/m has been drawn[1] and the steel coercivity has been measured. Figs. 3 and 4 show the distribution of the relative magnetic permeability $\mu_r \equiv \mu/\mu_0 = B/(\mu_0 H)$ at the nominal field of 1.55 T. Fig. 5 shows the relative magnetic permeability as a function of B for one particular sample (5976/A) of the slab steel, the return yoke steel (23921/B) and the steel produced by ILVA and used for the construction of the LNF prototype [4] [2]. The results

[1]The nominal magnetomotive force foreseen during data taking is 1600 A × 40 turns = 64000 A·turns corresponding to $H = 2864$ A/m.

[2]As a purpose of illustration, we plot samples 5976/A and 23921/B because their $\mu_r(B = 1.55T)$ are close to the mean value of $\mu_r(B = 1.55T)$ averaged over all samples.

can be summarized as follows.

- Due to the smaller Mn and C concentration the magnetic properties of the return yoke steel (RYS) are superior compared with the slab steel (SS). On average, the ratio of the relative permeabilities at B=1.55 T of RYS and SS is 1.67.
- The SS magnetic behaviour is extremely stable and non-uniformities in μ_r are of the order of 1%: $\mu_r(1.55T) = 476 \pm 6$.
- The smallness of the C concentration in the RYS makes difficult to keep under control local non-uniformities. The sample-by-sample variations are of the order of 12%: $\mu_r(1.55T) = 798 \pm 93$.
- For what concerns the slab steel, a better compromise between the mechanical and magnetic properties could have been obtained by reducing the Mn content and optimizing the procedure for mass production (e.g. reheating). This is demonstrated by the performance of the prototype steel (triangles in Fig.5), which retains appropriate mechanical properties but improves the magnetic response compared with the SS samples.

It is worth noting that both for RYS and SS the variations of $\mu_r(1.55T)$ between sample “A” and “B” are comparable with the variations among samples. In particular $\langle \mu_A - \mu_B \rangle = -0.5 \pm 84.4$ (RYS) and $\langle \mu_A - \mu_B \rangle = 5.6 \pm 5.1$ (SS). These non-uniformities in the same heat can have three different origins: errors in the measurements of μ_r at the permeameter, modifications of the steel properties during cut and machining of the sample and local variations of the magnetic properties of the steel. The first and the second systematic source should affect equally the RYS and SS measurements. On the other hand, a much higher dispersion of the measurements is observed for the RYS compared with SS. Therefore, the strong fluctuations of μ_r in the RYS are likely to be related to the smallness of the C concentration, which guarantees better magnetic response but compromises the steel uniformity or induces a higher sensitivity to the specific procedure followed during sample production.

4 Effect on the field strength and uniformity

The higher permeability of the return yoke steel compared with the slabs results into a slight reduction of the overall reluctance and, hence, an increase of the average field $\langle B \rangle$ along the magnetic circuit. On the other hand, non-uniformities and local fluctuations of B are expected, especially in the proximity of the return paths. A quantitative analysis of

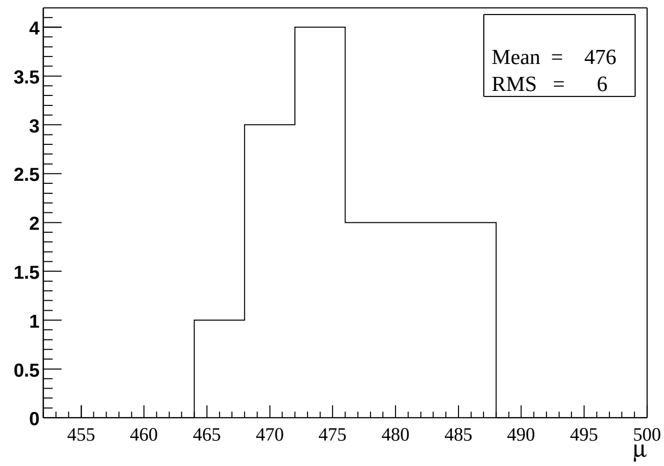

Figure 3: Distribution of the relative permeability $\mu_r(B = 1.55T)$ for the samples of the slab steel.

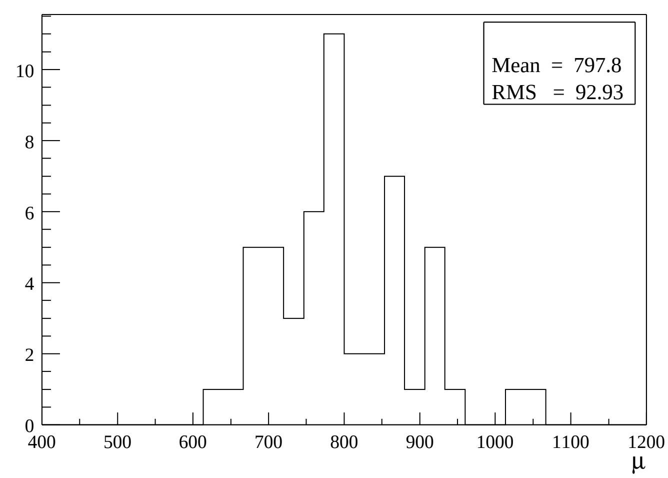

Figure 4: Distribution of the relative permeability $\mu_r(B = 1.55T)$ for the samples of the return yoke steel.

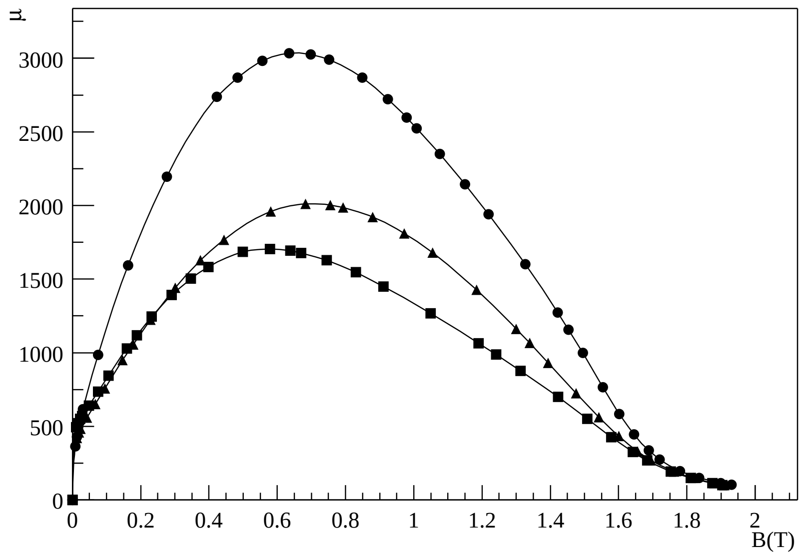

Figure 5: Relative permeability μ_r versus B for one sample of the slab steel (squares), the return yoke steel (circles) and the steel used for the construction of the prototype (triangles).

these effects has been carried out through finite-element calculation of the static B field at nominal magnetomotive force. The magnetostatic equations have been solved using the TOSCA code [5] and the spectrometer has been modeled using TOSCA pre-processor OPERA-3D. Three configurations have been considered:

- (Realistic): each return yoke (RY) block (see Fig. 12) has been simulated; the B-H curve of the steel is associated to the corresponding first magnetization curve (sample "A") as measured at CERN (see Sec.3); the B-H curve for the slab steel is that of the reference sample 5976/A.
- (Uniform RY): RY are assumed to be magnetically uniform and the B-H curve is taken from the reference sample 23921/B; the slabs are simulated as before.
- (Uniform magnet): the whole magnet is assumed to be uniform and the B-H curve is taken from the reference sample 5976/A.

In the reference frame defined for the simulation, the beam direction is labeled x, the vertical direction in Hall C is indicated with z and y represents the direction crossing all the RY blocks. Fig. 7 shows the value of $|\vec{B}|$ along y inside the lower return yoke (point "1" of Fig. 6). Figs. 8 and 9 show the field inside the steel at the center of 6^{th} slab and the field in air between the 5^{th} and 6^{th} slab (point "2" and "3" of Fig. 6, respectively).

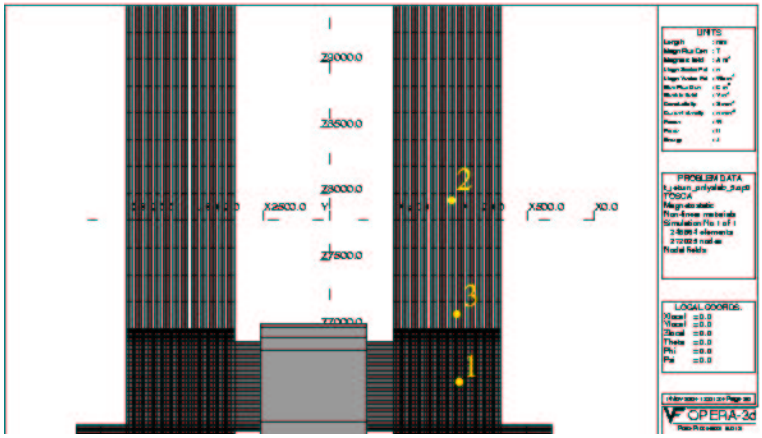

Figure 6: x and z coordinates of the field line plotted in Fig. 7 (position “1”), 8 (position “2”) and 9 (position “3”).

Figure 7: Absolute magnetic field $|\vec{B}|$ (in Tesla) along y inside the lower return yoke (see point “1” of Fig. 6) for the three configurations described in the text: Realistic (black), Uniform RY (red), Uniform magnet (green).

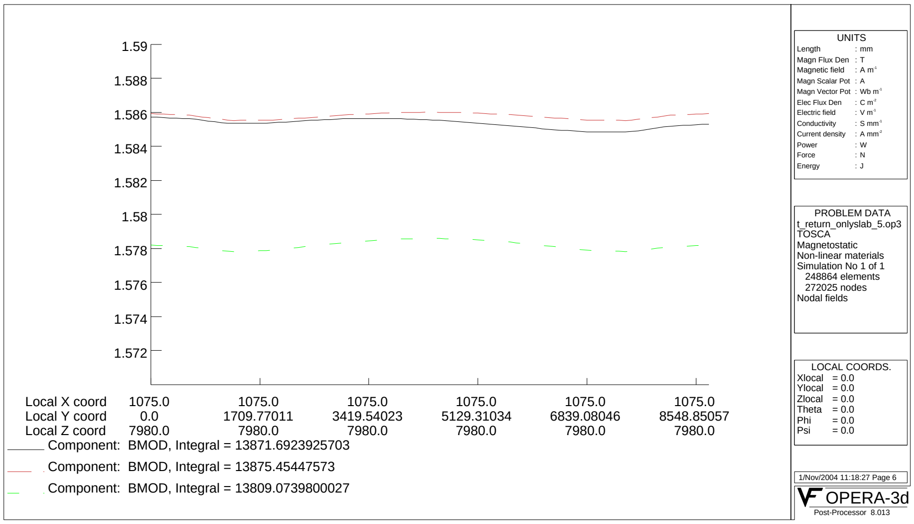

Figure 8: Absolute magnetic field $|\vec{B}|$ (in Tesla) along y at the center of the 6^{th} slab, 1 m above the lower return yoke (see point "2" of Fig. 6), for the three configurations described in the text: Realistic (black), Uniform RY (red), Uniform magnet (green).

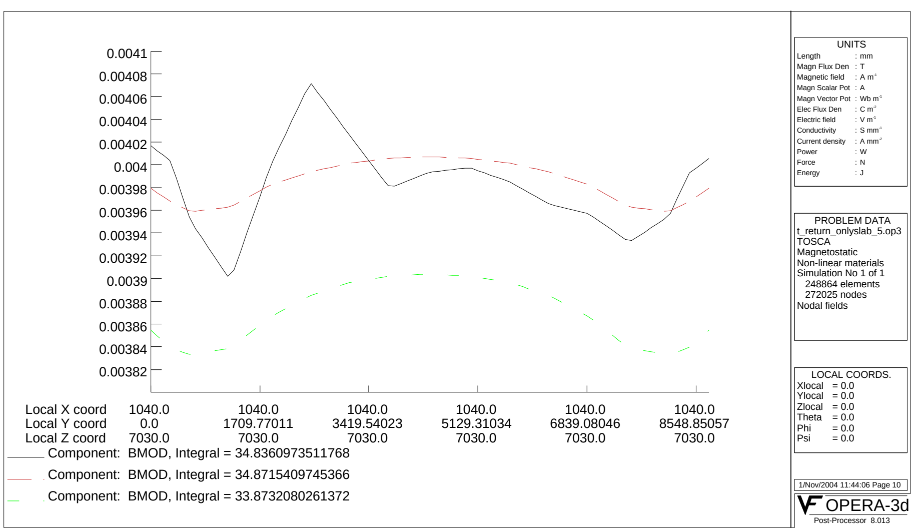

Figure 9: Absolute magnetic field $|\vec{B}|$ (in Tesla) along y in air between the 5^{th} and the 6^{th} slab, 3 cm above the return yoke (see point "3" of Fig. 6), for the three configurations described in the text: Realistic (black), Uniform RY (red), Uniform magnet (green).

The results of the simulation confirms the naive expectation discussed above and, in general, shows that the effect of non-uniformities and different magnetic properties between slabs and RY has a very limited impact to the physics performance of the spectrometer. More precisely, local variations of the field at the level of 10% are visible in the region of the RY but these non-uniformities are smoothed out in the active area of the spectrometer (vertical slabs). Local variations are already unobservable ($\ll 1\%$) 1 m above the RY. Moreover, the change of reluctance due to the better B-H curve of the RY compared with the slab steel results into a field variation of only $\sim$0.5% in the active area of the magnet (green line of Fig.8). The change of the fringe field in air is unobservable even by the Hall probes installed into the magnet air gaps. Therefore, for what concern the detector response the only effect that cannot be neglected is the increased systematic error ($\sim$10% compared with the nominal 3% [4]) in the knowledge of B for particles traversing the return yokes.

Finally, Fig. 10 shows the field along z at the center of slab 6 (the y coordinate corresponds to the middle of the spectrometer: 8750/2=4375 mm). Fields are computed assuming either the Realistic configuration (red line) or a hypothetical configuration where both the return yokes and the slabs are produced with the steel used for the construction of the prototype (black line). Again, the field difference does not exceed $\sim$1% since the large magnetomotive force foreseen during data taking (64000 A$\cdot$turns) brings the steel near the saturation regime, so that the discrepancies observed in Fig.5 (triangles versus squares) are washed out.

5 Conclusions

A rather detailed chemical and magnetic analysis of the steels for the OPERA spectrometer has been done during mass production and allowed a precise characterization of the magnetic circuit. Due to their different C and Mn content, the steels for the return yokes and for the slabs show opposite features: the former offers a higher magnetic quality but significant local non-uniformities; the latter, determining the field maps in the active region of the spectrometer, shows an extremely stable magnetic response but a lower permeability at fixed B. In general, this difference introduces additional systematics only for muons penetrating into the return yokes and, hence, it has a negligible impact on the physics performance of the detector. On the other hand, the expected strength and uniformity of the field in the sensitive region of the spectrometer (the one covered by the RPC's and the Drift Tubes) turns out to be well within the specifications indicated in the design phase of the experiment.

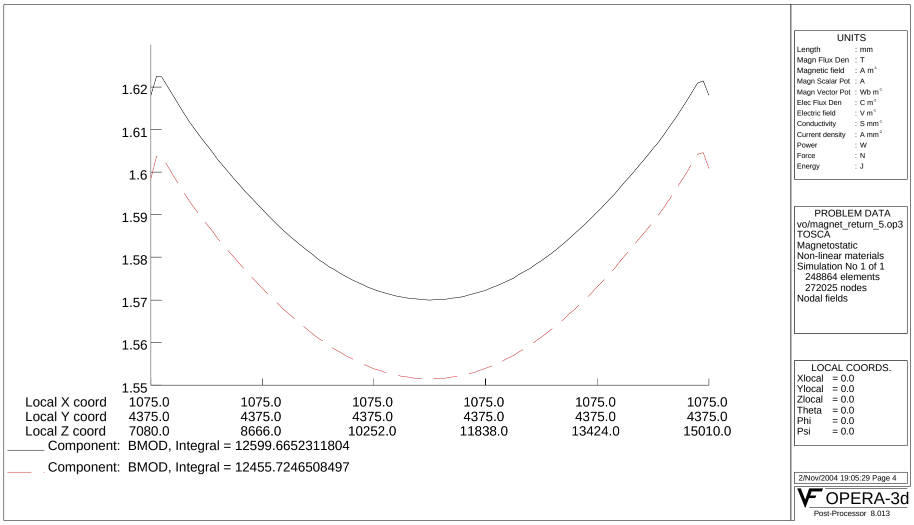

Figure 10: Absolute magnetic field $|\vec{B}|$ (in Tesla) along z (i.e. along the height) at the center of the 6^{th} slab for the Realistic configuration (red) or a hypothetical configuration where both the return yokes and the slabs are produced with the steel used for the construction of the prototype (black line).

Appendix A: Return yokes

The return yokes [3] are made up of six inner full blocks (width: 1250 mm; see Fig. 11) and two outer half-block (width: 625 mm) located as in Fig. 12. The half-block of the lower return yoke of the first (second) spectrometer are labeled A1,A8 (B1,B8). The corresponding blocks for the upper yoke are indicated with A1.S,A8.S (B1.S,B8.S). In this appendix we summarize the chemical analysis of the blocks, each block corresponding to a specific heat of the FOMAS steel. For every heat, three data sheets are available: the ladle analysis done by the steel maker (labeled "SM") and the analysis done for the two samples extracted from the heat (samples "A" and "B"). For these samples we provide also the relative magnetic permeability at B=1.55 T as measured by the steel producer (μ_1) and by one of us (G.P.) at CERN (μ_2) together with the coercivity ("Coer"). Note that the measurements done by the steel maker are systematically lower than that of CERN by about 8%. The data are summarized in Tables 2, 3, 4, 5. The weight fractions are expressed in units of 10^{-5} and the coercivity in A/m.

Sample	Position	Type	C	Si	Mn	P	S	B	μ_1	μ_2	Coer
23809	A2	SM	5	865	219	4	8	0.2			
23809	A2	A	5	869	222	4	7	0.2	896	916	103
23809	A2	B	4	872	217	5	8	0.2	758	779	115
23810	A3	SM	8	800	210	2	2	0.2			
23810	A3	A	8	805	217	2	2	0.2	783	790	86
23810	A3	B	7	811	213	3	2	0.2	705	679	73
23811	A4	SM	3	875	211	2	7	0.2			
23811	A4	A	3	879	219	3	6	0.2	658	679	104
23811	A4	B	4	883	220	2	6	0.2	762	757	108
23812	A5	SM	4	857	276	5	3	0.2			
23812	A5	A	4	863	282	4	3	0.2	828	856	117
23812	A5	B	4	859	285	5	2	0.2	794	924	89
23849	A6	SM	3	801	250	3	8	0.1			
23849	A6	A	3	805	248	4	8	0.1	851	784	73
23849	A6	B	4	811	255	3	8	0.1	640	766	76
23850	A7	SM	2	824	225	3	6	0.2			
23850	A7	A	3	832	229	3	7	0.1	751	751	81
23850	A7	B	2	826	233	3	6	0.1	785	778	88
23851	A1	SM	4	999	231	2	1	0.2			
23851	A1	A	5	1020	236	3	1	0.1	824	840	80
23851	A1	B	4	995	239	2	2	0.1	924	907	72
23852	A8	SM	8	830	250	3	8	0.1			
23852	A8	A	9	834	258	4	7	0.1	651	770	82
23852	A8	B	8	837	262	3	8	0.1	630	795	90

Table 2: Chemical and magnetic analysis of the lower return yoke blocks of the first spectrometer (see text for details). The weight fractions are expressed in units of 10^{-5} and the coercivity in A/m.

Sample	Position	Type	C	Si	Mn	P	S	B	μ_1	μ_2	Coer
24321	A4.S	SM	3	841	214	6	8	0.2			
24321	A4.S	A	3	845	218	6	8	<0.1	919	869	74
24321	A4.S	B	2	849	223	7	8	<0.1	882	1045	73
24322	A6.S	SM	3	877	248	2	7	0.2			
24322	A6.S	A	4	882	255	2	8	<0.1	597	697	71
24322	A6.S	B	3	878	246	3	7	<0.1	735	876	72
24323	A3.S	SM	7	838	228	4	7	0.2			
24323	A3.S	A	6	842	234	5	7	<0.1	658	859	74
24323	A3.S	B	7	846	237	4	6	<0.1	760	858	78
24324	A5.S	SM	3	841	214	6	8	0.2			
24324	A5.S	A	3	809	223	5	6	<0.1	833	missing	
24324	A5.S	B	2	812	217	4	5	<0.1	865	missing	
24327	A1.S	SM	3	841	214	6	8	0.2			
24327	A1.S	A	8	841	262	2	8	<0.1	720	769	111
24327	A1.S	B	10	827	259	3	9	<0.1	648	713	107
24328	A8.S	SM	4	999	231	2	1	0.2			
24328	A8.S	A	6	984	237	2	2	<0.1	657	698	93
24328	A8.S	B	5	996	243	2	1	<0.1	858	1037	78
24325	A2.S	SM	3	809	300	4	8	0.2			
24325	A2.S	A	4	814	307	4	9	<0.1	805	missing	
24325	A2.S	B	2	818	312	4	8	<0.1	805	missing	
24326	A7.S	SM	3	841	214	6	8	0.2			
24326	A7.S	A	4	830	222	5	4	<0.1	865	missing	
24326	A7.S	B	3	821	219	6	3	<0.1	993	missing	

Table 3: Chemical and magnetic analysis of the upper return yoke blocks of the first spectrometer (see text for details). The weight fractions are expressed in units of 10^{-5} and the coercivity in A/m.

Sample	Position	Type	C	Si	Mn	P	S	B	μ_1	μ_2	Coer
23920	B4	SM	9	850	204	5	2	0.2			
23920	B4	A	8	855	212	5	3	0.1	660	missing	
23920	B4	B	9	859	208	4	2	0.1	628	missing	
23921	B5	SM	5	846	216	5	9	0.2			
23921	B5	A	4	852	219	5	8	0.1	722	798	110
23921	B5	B	6	849	217	5	9	0.1	702	780	110
23922	B3	SM	2	829	231	2	9	0.2			
23922	B3	A	2	834	231	3	9	0.1	670	687	103
23922	B3	B	4	838	236	2	8	0.1	600	614	122
23923	B6	SM	3	903	214	1	7	0.2			
23923	B6	A	2	906	219	2	8	0.1	641	689	98
23923	B6	B	4	913	222	1	7	0.1	596	643	102
23924	B2	SM	3	935	269	2	10	0.3			
23924	B2	A	2	938	274	1	9	0.1	642	702	84
23924	B2	B	4	944	267	2	9	0.1	581	691	89
23925	B7	SM	8	833	211	2	4	0.1			
23925	B7	A	7	837	220	2	4	0.1	619	711	95
23925	B7	B	8	841	217	1	4	0.1	662	706	99
24084	B1	SM	5	812	200	4	6	0.2			
24084	B1	A	5	822	208	4	7	0.1	645	731	83
24084	B1	B	6	819	211	4	6	0.1	675	738	84
24085	B8	SM	7	878	242	4	8	0.1			
24085	B8	A	9	884	249	5	8	0.1	625	728	91
24085	B8	B	7	888	245	4	7	0.1	630	697	101

Table 4: Chemical and magnetic analysis of the lower return yoke blocks of the second spectrometer (see text for details). The weight fractions are expressed in units of 10^{-5} and the coercivity in A/m.

Sample	Position	Type	C	Si	Mn	P	S	B	μ_1	μ_2	Coer
24452	B4.S	SM	2	967	228	3	6	0.1			
24452	B4.S	A	4	955	234	4	7	<0.1	878	880	99
24452	B4.S	B	3	971	224	2	6	<0.1	750	777	93
24453	B5.S	SM	9	953	216	3	3	0.1			
24453	B5.S	A	10	962	229	2	3	<0.1	840	888	63
24453	B5.S	B	8	960	218	3	4	<0.1	1055	1024	94
24454	B3.S	SM	7	930	298	4	4	0.1			
24454	B3.S	A	7	937	306	5	5	<0.1	898	931	71
24454	B3.S	B	8	940	306	5	4	<0.1	705	801	85
24455	B6.S	SM	8	816	269	5	6	0.1			
24455	B6.S	A	7	823	275	4	6	<0.1	880	954	81
24455	B6.S	B	9	818	281	5	7	<0.1	840	932	91
24513	B2.S	SM	8	821	300	9	1	0.1			
24513	B2.S	A	9	832	305	10	2	<0.1	695	786	88
24513	B2.S	B	8	828	313	8	1	<0.1	680	791	78
24514	B7.S	SM	4	808	280	11	2	0.1			
24514	B7.S	A	6	815	291	10	1	<0.1	730	762	95
24514	B7.S	B	5	820	284	12	2	0.1	695	791	73
24515	B1.S	SM	5	812	200	4	6	0.2			
24515	B1.S	A	5	818	207	5	6	<0.1	735	817	78
24515	B1.S	B	7	832	213	4	7	<0.1	735	840	83
24516	B8.S	SM	7	878	242	4	8	0.1			
24516	B8.S	A	9	885	253	5	8	<0.1	730	858	96
24516	B8.S	B	7	884	248	3	8	<0.1	715	757	96

Table 5: Chemical and magnetic analysis of the upper return yoke blocks of the second spectrometer (see text for details). The weight fractions are expressed in units of 10^{-5} and the coercivity in A/m.

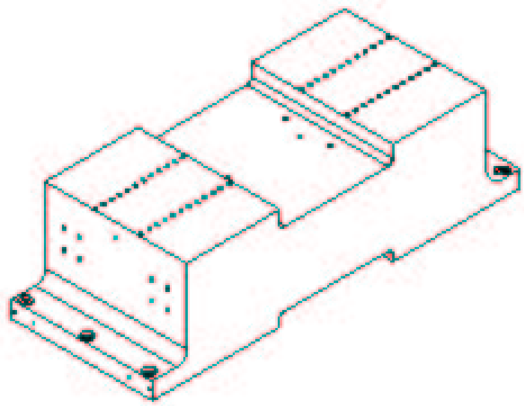

Figure 11: A full block belonging to the lower return yoke of the magnet.

Appendix B: Slabs

Fourteen toroidal samples (two per heat) have been extracted from the steel used for the slab mass production. The samples belonging to the same heat are labeled “A” and “B” and in Table 6 we provide the relative magnetic permeability at B=1.55 T (measured at CERN) and the coercivity. No magnetic measurements have been done by the steel producers. The last row of the Table (label “proto”) describes the steel produced by ILVA for the construction of the LNF magnet prototype [4] .

References

[1] M. Ambrosio et al., IEEE Trans. Nucl. Sci. **51** (2004) 975.

[2] M. Guler et al. [OPERA Collaboration], CERN/SPSC 2000-028, SPSC/P318, LNGS P25/2000; M. Guler et al. [OPERA Collaboration], CERN/SPSC 2001-025, SPSC/M668, LNGS EXP30/2001 Add. 1/01, Aug. 2001.

[3] D. Autiero (ed.), “The OPERA Technical Design Report”, in preparation.

[4] G. Di Iorio et al., “Measurements of Magnetic Field in the Prototype of the OPERA Spectrometer”, LNF-01/028(IR).

[5] OPERA-3d OPERA-2d and TOSCA are products by Vector Field Ltd., Oxford, UK (www.vectorfields.co.uk).

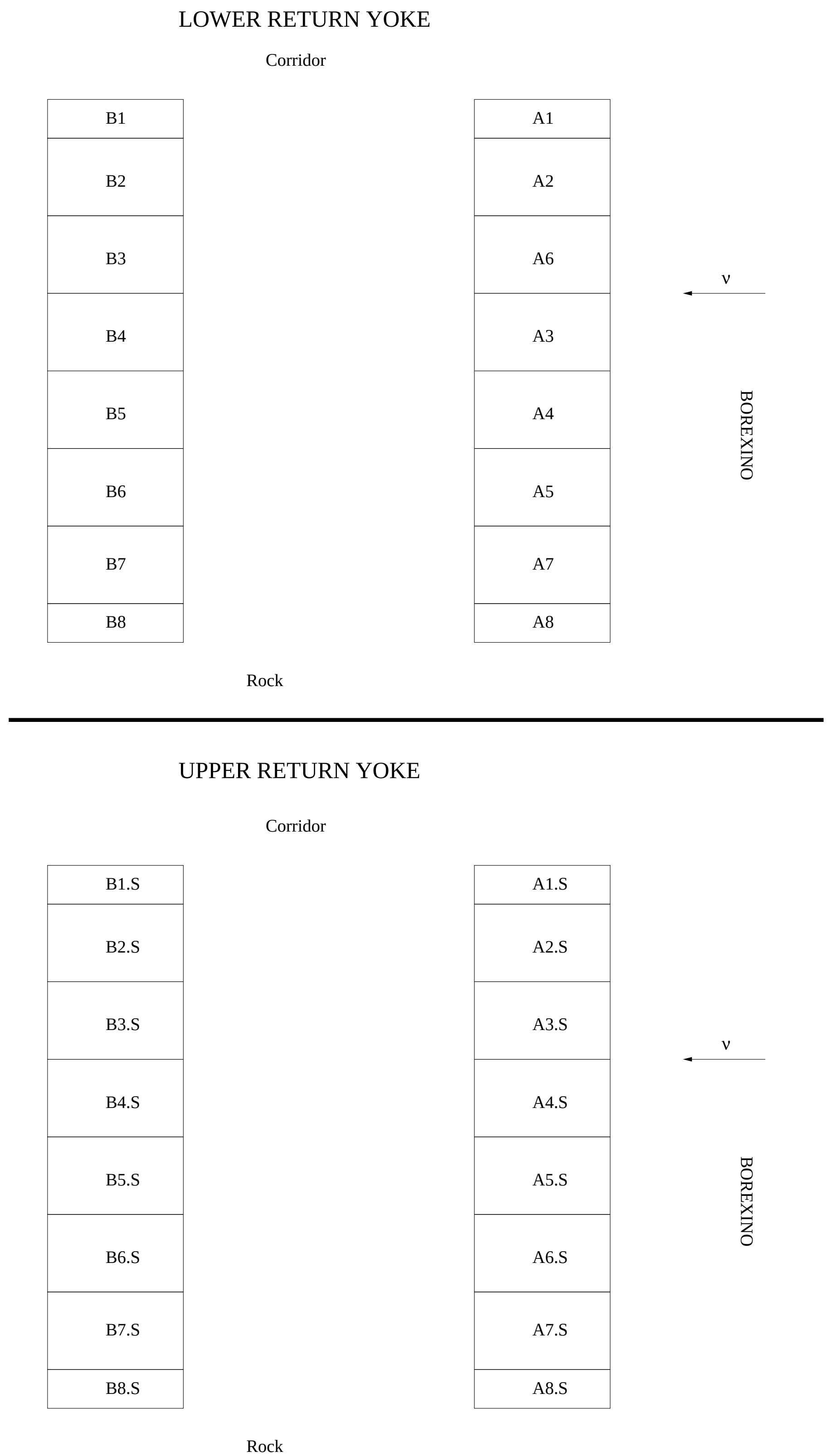

Figure 12: Position of the blocks for the upper and lower return yokes of the first (A) and second (B) spectrometer.

Sample	Type	μ_r(B=1.55T)	Coercivity (A/m)
5843	A	475.35	169.54
5843	B	469.88	171.33
5856	A	480.86	168.82
5856	B	472.21	169.87
5872	A	484.88	166.54
5872	B	472.76	169.91
5937	A	471.51	169.33
5937	B	466.19	174.86
5945	A	475.17	167.96
5945	B	478.78	169.96
5962	A	484.14	168.98
5962	B	481.45	168.93
5976	A	477.80	172.02
5976	B	469.36	172.83
proto	-	545.25	179.34

Table 6: Magnetic properties of the slab steel. The label “proto” refers to the steel used for the construction of the LNF prototype.